

BODIPYs α -appended with distyryl-linked aryl bisboronic acids: single-step cell staining and turn-on fluorescence binding with D-glucose

Received 00th January 20xx,
Accepted 00th January 20xx

DOI: 10.1039/x0xx00000x

Adil Alkaş,^a Joshua M. Kofsky,^b Em C. Sullivan,^a Daisy Nebel,^b Katherine N. Robertson,^c Chantelle J. Capicciotti,^b David L. Jakeman,^{a,d} Erin R. Johnson,^a and Alison Thompson^{a*}

Small-molecule sensors that are selective for particular sugars are rare. The synthesis of BODIPYs appended with two boronic acid units is reported, alongside cellular staining/labelling and turn-on fluorescence binding data for carbohydrates. The structural frameworks were designed using computational methods, leaning on the chelation characteristics of bis(boronic acids) and the photophysical properties of BODIPYs. Selective binding to glucose is demonstrated via emission and absorption methods, and the challenges of using NMR data for studying carbohydrate binding are discussed. Furthermore, crystal structures, cell permeability and imaging properties of the BODIPYs appended with two boronic acid units are described. This work presents boronic-acid-appended BODIPYs as a potential framework for tunable carbohydrate sensing and chemical biology staining.

Introduction

Carbohydrates are abundant in living systems and play crucial roles in physiological and pathological processes.^{1–4} The ability to accurately detect and quantify carbohydrates is vital to the diagnosis of disease. Indeed, detection of certain types of cell surface carbohydrates is important for the diagnosis of correlated cancers.^{5–8} Similarly, the accurate measurement of blood glucose levels is critical for the diagnosis and management of diabetes.^{9,10}

Techniques for monitoring blood glucose levels typically involve enzyme-catalyzed electrochemical reactions.^{9,10} For example, the oxidation of D-glucose, catalyzed by glucose oxidase, generates D-gluconolactone and hydrogen peroxide. The concentration of D-glucose can thus be assessed via the consumption of oxygen, the production of hydrogen, or the production of gluconic acid formed from D-gluconolactone.^{9,11} However, enzyme-based methods have practical limitations such as the stability of the enzyme, the necessity of a blood sample, and various calibration requirements.^{9,11} Small-molecule fluorescent sensors offer tunable chemical frameworks with the potential for greater stability, high optical

sensitivity and rapid analytical responses.^{6,12–14} However, despite the increasing number of reports in this area,¹⁵ many small-molecule sensors are described without convincing structural or binding data,^{16,17} and most rely on detection instrumentation that is impractical for translation into a portable device for patients. For example, evidence of binding to glucose and fructose for an iridium(III)-boronic acid system consisted of only mass spectrometry data.¹⁸ Similarly, some reports have highlighted the glucose selectivity of cyclodextrin-fluorophore sensors based on circular dichroism and/or fluorescence measurement data without rationale for the nature of the glucose binding in these complex multicomponent systems.^{19,20} Some reports have focused on electrohydrodynamic²¹ and electrochemical²² sensing systems as an alternative to conventional enzymatic electrochemical sensing methodology, while others have suggested using nuclear magnetic resonance (NMR) spectroscopy for glucose detection.^{23–25} Moreover, several reports have described nanoparticle-based glucose-sensing systems that are unsuitable for use in oxygen-rich environments.^{26–28} In this respect, characterising small-molecule sensor-glucose binding/interactions and optimising detection techniques remain crucial for developing optimal sensors for carbohydrates.

Boronic acids have attracted attention within the realm of glucose sensing due to their ability to form reversible covalent bonds with cis-1,2- and cis-1,3-diols.^{9,11,14,29–31} A variety of sensor systems containing boronic acids have been reported, including small-molecule, polymeric and nano-material-based systems.^{32,33} Yet, the design of sensors with selectivity for glucose remains a challenge due to the structural similarity of many monosaccharides.³⁰ Generally, sensors bearing monoboronic acids demonstrate selectivity for fructose over

^a Department of Chemistry, Dalhousie University, Halifax, Nova Scotia, B3H 4J3, Canada.

^b Department of Chemistry, Queen's University, Kingston, Ontario, K7L 3N6, Canada.

^c Department of Chemistry, Saint Mary's University, Halifax, Nova Scotia, B3H 3C3, Canada.

^d College of Pharmacy, Dalhousie University, Halifax, Nova Scotia B3H 4R2, Canada

† Footnotes relating to the title and/or authors should appear here.

Electronic Supplementary Information (ESI) available: [details of any supplementary information available should be included here]. See DOI: 10.1039/x0xx00000x

glucose and other monosaccharides.³⁰ The identification of sensor systems with improved binding affinity to glucose has been achieved by using diboronic acids. James *et al.* reported a fluorescent turn-on glucose sensor based on an anthracene framework bearing two boronic acid sites.³⁴ The spacer between the two boronic acids was demonstrated to play a crucial role for glucose recognition.^{35,36} This work was followed by reports of a number of carbohydrate sensors containing two boronic acids.^{37–42} For example, a structurally more rigid sensor system containing the diboronic acid motif was reported by Drueckhammer *et al.* (Figure 1), with the design relying on computational approaches and geometry optimisation.⁴³ Despite its high selectivity for glucose over galactose, mannose or fructose, this system provided turn-off fluorescence behaviour upon glucose binding.

A critical element of a small-molecule carbohydrate sensor system is the reporting moiety, e.g. a fluorophore. BODIPYs (4,4-disubstituted-4-bora-3a,4a-diaza-s-indacenes) are generally stable organic fluorophores with strong absorption and high fluorescence quantum yields.^{44,45} The BODIPY core has multiple sites (α , β and *meso* positions, and the boron center) at which structural derivatisation may be employed in order to tune photophysical properties.^{44,46} However, there are only a handful of reports focusing on the use of BODIPY dyes in carbohydrate sensing. These BODIPY-based sensors feature boronic acids at the *meso* position^{47–52} or at the α - and β -positions,^{22,53,54} although one system binds sugars directly at the boron center of the BODIPY core.^{55,56} It is known that BODIPYs featuring monoaryl boronic acid substituents recognise saccharides with fluorescence enhancement.^{48,50–52} Here, new bisboronic acid-based glucose probes featuring the BODIPY core are presented. Derivatisation through the 3,5-positions, by installing styryl substituents, results in conformationally rigid structures with absorption and emission behaviour reaching wavelengths of ~ 650 nm.^{57–60} Furthermore, the system is open to chemical modification through the aryl groups, thus enabling tuning of properties such as the emission profile, binding and solubility.

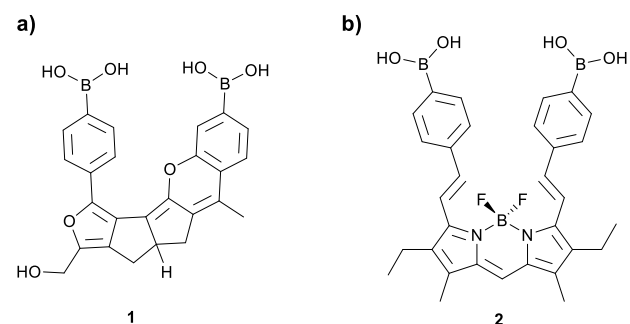


Figure 1 Structures of a) glucose receptor **1** reported by Drueckhammer and b) new BODIPY-based bisboronic acid **2**.

Results and discussion

DFT calculations

The three-dimensional architectures presented by bisboronic acids play an important role in preferential binding to a particular carbohydrate.⁶¹ Inspired by Drueckhammer's sensor **1** (Figure 1), DFT calculations were used to explore 1:1 sensor:glucose binding modes of BODIPYs α -appended with distyryl-linked aryl bisboronic acids. The incorporation of rigid distyryl units at the α -positions provides a framework that mimics Drueckhammer's system.⁴³ To the best of our knowledge, there is only one report of a distyryl-appended BODIPY with two boronic acid moieties used in glucose sensing.²² However, this sensor relies on an electrochemical signal rather than on fluorescence emission. By altering the position of each boronic acid on the pendent aryl rings, the para-substituted system **2** and the meta-substituted **3** were considered (Figure 1 and Figure 2). Geometries for the 1:1 BODIPY:glucose complexes were optimised using the LC- ω BPE density functional⁶² with XDM dispersion correction,^{63,64} following Drueckhammer's approach, optimisations focussed on α -D-glucopyranose, complexed to the two boronic atoms through the 1,2- and 4,6-positions. The methyl and ethyl substituents were omitted in the DFT calculations, for simplicity (see SI for further details). The optimised structures of complex-**2'** and that reported by Drueckhammer show considerable geometrical overlap, as shown in Figure S17. According to calculation, the meta-substituted diboronic acid **3** is the most favourable binder (complex-**3'**), with a relative binding energy of -2.3 kcal/mol compared to the previously reported **1** (0.0 kcal/mol for complex-**1'**) and the para-substituted diboronic acid **2** (6.4 kcal/mol for complex-**2'**).

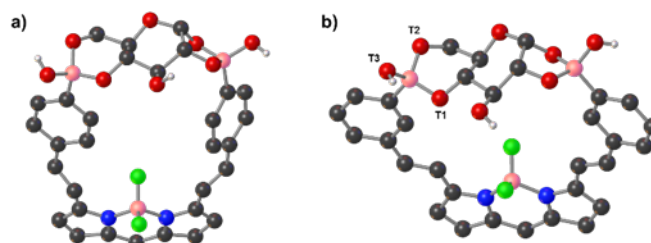
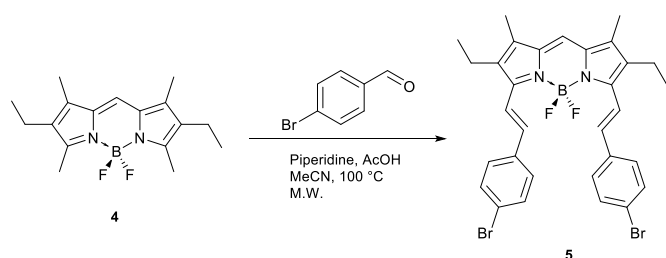


Figure 2 Optimised structures of (a) complex-**2'** and (b) complex-**3'**. Hydrogen atoms bonded to carbon are omitted for clarity.

Synthesis and characterisation

In order to prepare the desired BODIPY-appended bisboronic acids **2** and **3**, a synthetic route involving Knoevenagel condensation was envisaged. Compound **5** was used as a model substrate with which to establish reaction conditions (Scheme 1; Table S1).^{65,66} The reactions were performed using microwave-promoted conditions, and progress was monitored by using TLC. The effect of solvent and catalyst were studied first. Three new spots were observed on TLC when the reaction was performed in MeCN and a mixture of piperidine:acetic acid was used as the catalyst (Table S1a). Replacing the solvent with DMF resulted in a more complex product mixture, and varying the amounts of piperidine and acetic acid was also unproductive

(Table S1b-S1e). Enhanced conversion to the desired product was observed when the reaction time was increased to 1 hour (Table S1f), and consequent purification via column chromatography on silica provided the desired compound **5**. Increasing the reaction time to 2 hours did not result in improved product yield, according to TLC analysis, while after 3 hours the formation of new undesired spots was observed (Table S1g). A higher yield was obtained when the amount of 4-bromobenzaldehyde was increased (Table S1h). Conditions involving the use of molecular sieves (3 Å) for the Knoevenagel condensation had previously been shown to enhance substitution of BODIPYs at the 3- and 5-positions.⁵⁷ However, the presence of molecular sieves in the reaction shown in Scheme 1 lowered the product yield (Table S1i).



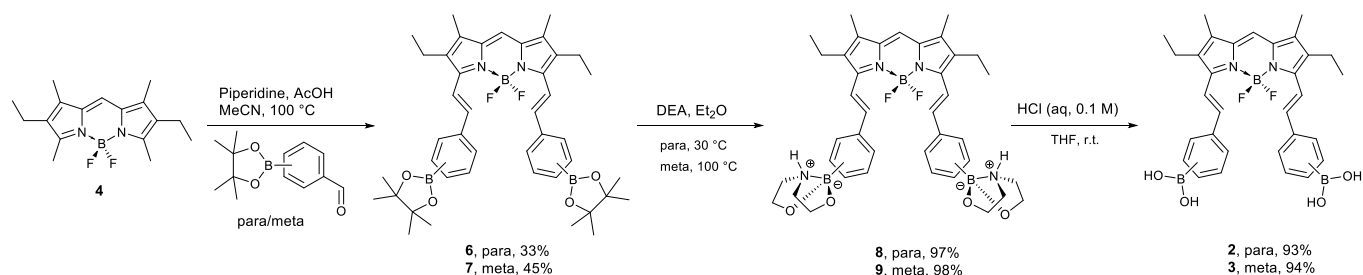
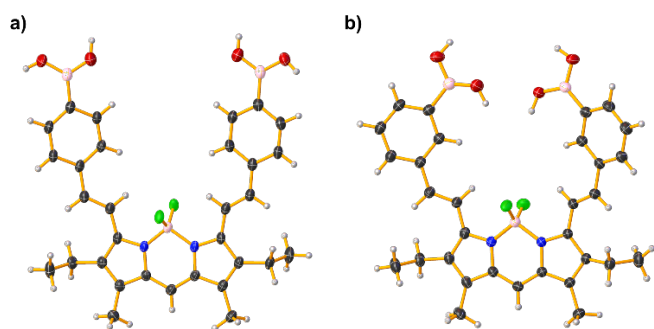
Scheme 1 Synthesis of compound **5**.

The optimal reaction conditions (4 eq. of aldehyde; MeCN; no molecular sieves) were applied to the synthesis of the target pinacol esters **6** and **7** using benzaldehydes featuring pinacol ester substituents at the para- and meta-positions (Scheme 2). The materials isolated after column chromatography were semi-pure and thus washed with pentane to provide the desired products. Compounds **6** and **7** were also isolated in moderate yield when the reactions were conducted via use of conventional heating in a glass pressure-vessel (Supporting Information, pages S9 and S12, respectively). Next, the hydrolysis of pinacol-protected boronate esters **6** and **7** to their corresponding boronic acids **2** and **3**, respectively, was explored (Scheme 2). Among several previously reported methods by which to deprotect boronate esters,^{67–70} transesterification with diethanolamine (DEA) and hydrolysis of the corresponding DEA ester was noted to require only mild reaction conditions.⁷¹ Thus, stirring a solution of **6** in diethyl ether with DEA at room temperature overnight was attempted, resulting in complete conversion of **6** to the DEA-based ester **8**. However, the reproducibility of this reaction was found to vary drastically as a result of slight changes in the room temperature caused by seasonal effects. The lower temperatures presumably reduced the solubility of the intermediate (the mono salt), such that this material precipitated from the reaction mixture and further

deprotection was limited. Reliable and complete conversion of **6** to **8** was achieved by conducting the reaction at 30 °C, whilst the synthesis of **9** required higher temperatures and reaction times. Indeed, heating a solution of **7** in diethyl ether with DEA at 100 °C in a sealed glass pressure-vessel for two days produced the DEA-based ester **9** in excellent purity and isolated yield.

Hydrolysis of the ester **8** was initially attempted in 1 M HCl, with THF as a co-solvent: however, starting material remained even after stirring overnight at room temperature. The use of diethyl ether as a co-solvent alongside 1 M HCl resulted in complete consumption of the starting material, and the production of several decomposition products. Finally, the reaction was conducted using 0.1 M HCl/THF. The desired diboronic acid **2** was thus obtained in high yield after only 1 h, reproducible on larger scales. This synthetic protocol was also applied to the hydrolysis of ester **9** to generate the desired diboronic acid **3**. All compounds were characterised by ¹H, ¹³C, ¹¹B and ¹⁹F NMR spectroscopy, mass spectrometry, and UV-vis and fluorescence techniques.

Crystals of **2**, **3**, **5**, **6** and **7** of suitable quality for X-ray diffraction were grown by slow evaporation of solutions involving dichloromethane for **5**, MeCN for **6** and **7**, and a mixture of MeCN:H₂O for **2** and **3**. The crystal structures of these compounds are shown in Figure 3 and Figures S61-S83. In each of the structures, the BODIPY cores feature an approximately planar backbone and the boron atoms are coordinated in a tetrahedral geometry with two dipyrinato nitrogen atoms and two fluorine atoms. The relative planarity of these molecules allows them to pack in layered arrangements. Systems of H-bonds form between molecules within the same plane and solvent located in the associated cavity. Stacking interactions also form between the aromatic rings in molecules in differing layers. These two features, working in concert, offer appreciable crystal lattice stabilisation. However, bringing the molecules sufficiently close to interact also results in clashes of the pendent boron-containing groups. This results in the disorder observed in the structures and/or the twisting of the styryl groups away from the plane, to minimise the clashes. This rotation, in turn, diminishes the stacking and weakens the hydrogen bonding. These observations are compatible with previous literature reports on similar BODIPY derivatives.^{72–74} As shown in Figure 3, the vinyl substituent of the styryl groups are in the *trans* configuration anticipated for the diboronic acids **2** and **3**. Additionally, the structures of **2** and **3** each reveal H-bonded dimers joined between boronic acid groups on neighbouring molecules (Figure S74 and S81, respectively). The cavity enclosed by the dimer contains solvent, i.e. CH₃CN in **2** and CH₃CN/H₂O in **3**, which also participates in and strengthens the H-bonded network.

Scheme 2 Synthetic route to bisboronic acids **2** and **3**.Figure 3 X-ray structures of **2** (a) and **3** (b). Thermal ellipsoids have been drawn at the 50% probability level. Disorder and solvent molecules were removed for clarity.

The absorption and emission properties for **4-7** were measured in CH_2Cl_2 whereas DMSO was used for compounds **2**, **3**, **8** and **9**, based on their optimal solubilities. With extinction coefficients (ϵ) of 70-100,000 $\text{M}^{-1} \text{cm}^{-1}$ (Table 1) at maximal absorption wavelengths ($\lambda_{\text{abs}}^{\text{max}}$), the absorption spectra of compounds **2-3** and **5-9** feature similar strong bands at 600-750 nm (Figure 4), and matching their deep blue colour. These characteristics agree with absorption profiles of previously reported distyryl BODIPY derivatives.^{44,46,57}

Compounds **2-9** emit at wavelengths in the orange/red visible region (Figure 4) with Stokes shifts (S.S.) for maximal emission wavelengths ($\lambda_{\text{em}}^{\text{max}}$) in the range of 13-18 nm (Table 1). The quantum yield of fluorescence (Φ_f) for compound **5** in CH_2Cl_2 was 0.51, while pinacol esters **6** and **7** exhibited higher quantum yield values of 0.61 and 0.64, respectively. The DEA-based esters and the boronic acids exhibited lower quantum yields compared to their corresponding pinacol esters, ranging from 0.33-0.49 (in DMSO).

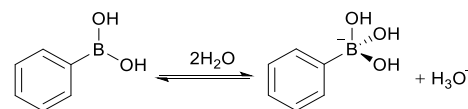
pKa Determination

The acidity of boronic acids lies in their Lewis acid characteristics due to the vacant p-orbital of boron in the

Table 1 Photophysical properties of compounds **2-9**

Compound	Solvent	$\lambda_{\text{abs}}^{\text{max}}$ (nm)	ϵ ($\text{M}^{-1} \text{cm}^{-1}$)	$\lambda_{\text{em}}^{\text{max}}$ (nm)	S. S. (nm)	Φ_f
4	DCM	530	59900	539	9	0.96
5	DCM	652	87800	665	13	0.51
6	DCM	656	100200	669	13	0.61
7	DCM	648	107900	661	13	0.64
8	DMSO	656	70200	673	17	0.33
9	DMSO	652	83000	669	17	0.33
2	DMSO	652	75900	668	16	0.49
3	DMSO	644	71100	662	18	0.34

trigonal (sp^2 hybridised) form. The trigonal form is transformed into the tetrahedral boronate ion (sp^3 hybridised) upon complexation with hydroxide (Scheme 3).⁷⁵ The pKa value of a boronic acid is defined as the pH at which 50% of the boronic acid exists as the tetrahedral-boronate ions.⁷⁶ As tetrahedral boronate has a superior tendency to form cyclic boronate esters, compared to neutral boronic acids,^{77,78} the pKa value is an important parameter for carbohydrate sensing.



Scheme 3 The acid-base equilibrium of phenylboronic acid.

Attempts to determine the pKa value of diboronic acid **2** were complicated by its limited solubility at lower pH values. The pKa value of **3** was determined to be 10.8 by monitoring the change in absorbance as a function of pH in 35% DMSO phosphate buffer (Figure S39-40). The pKa value found for **3** is higher than those reported for common aryl boronic acids, albeit those values are often measured in aqueous buffers.^{76,79} Computational studies have predicted the pKa of some aryl boronic acids in DMSO to be much higher than their

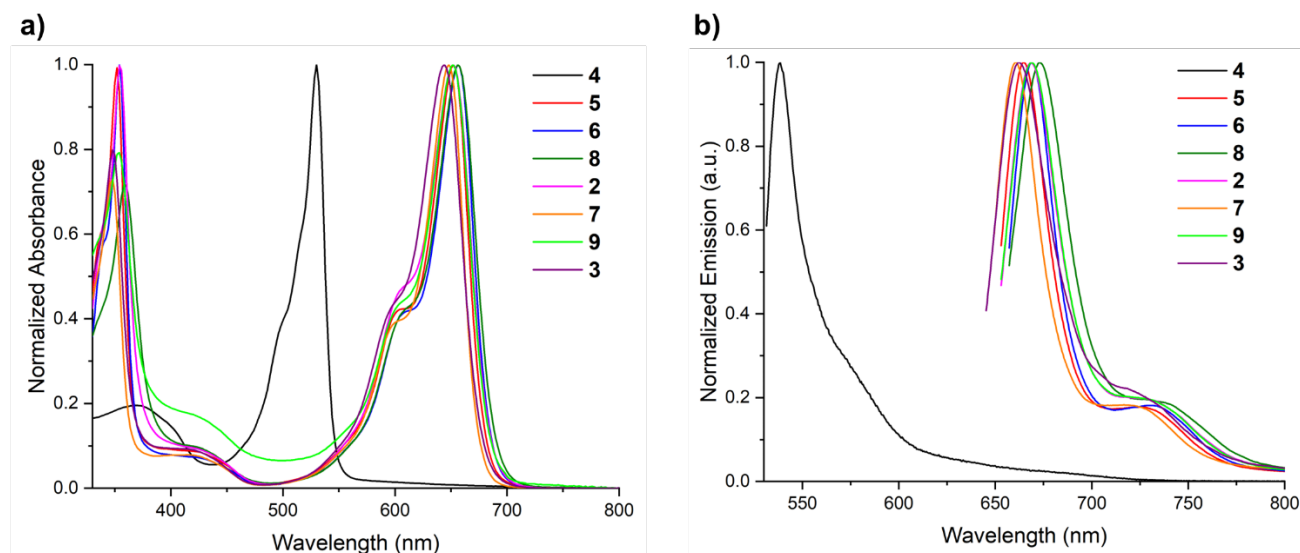


Figure 4 Normalised absorbance (a) and emission (b) spectra of compounds 2-9.

corresponding acidities in aqueous solution.⁸⁰ Nevertheless, the properties of bisboronic acid **3** are as anticipated and suggest the required characteristics for binding to carbohydrates.

Carbohydrate Titration Experiments

To explore the carbohydrate binding abilities of BODIPYs **2** and **3** α -appended with distyryl-linked aryl diboronic acids, their solubility in phosphate buffer solutions was evaluated.^{38,81} In the absence of an organic co-solvent, both compounds are insoluble in acidic and basic phosphate buffer and adding up to 20% acetonitrile did not result in dissolution. Further increasing the amounts of acetonitrile caused the precipitation of buffer salts. Changing the co-solvent from acetonitrile to methanol improved the solubility of the two dyes in the buffered solutions, but subsequent titrations highlighted the capricious solubility of the dyes at even slightly varying temperatures and even with high methanol concentrations (up to 80% methanol in 0.012 M phosphate buffer). Although **2** precipitated rapidly from 20-35% DMSO in 0.012 M phosphate buffer solutions at pH values ranging from 7.5 to 9, solutions of pH 10 remained fully dissolved. However, a slow decrease in the fluorescence intensity of diboronic acid **2** (3.3 μ M) in 35% DMSO/0.012 M phosphate buffer solutions at pH 10 was observed over a period of 4 hours (Figure S27). As such, timely experiments were conducted with a buffer of this composition to explore the effects of complexation between **2** and D-glucose on the stability of the solution.

When **2** was titrated with increasing amounts of D-glucose in 35% DMSO/0.012 M phosphate buffer at pH 10, a slight

increase in the absorbance and fluorescence intensities was observed (Figures S41-42), supporting the presence of a weak interaction between **2** and D-glucose. As noted above, DFT calculations suggested a lower binding energy for complex-**2** than complex-**3** and so subsequent investigations focused on the meta-substituted analogue **3**. The blue solution of **3** in 20% DMSO/0.012 M phosphate buffer exhibited a strong emission band at 660 nm when excited at 645 nm. Fluorescence enhancement was observed upon addition of D-glucose (3.3 mM), and the intensity of this sample increased over a period of 20 minutes, then started to decrease (Figure S29 and S30). The fluorescence of **3** in 35% and 50% DMSO/buffer solutions were stable for one hour and four hours, respectively (Figure S31 and S34). Although higher percentages of DMSO improved the solubility of **3**, no change was observed in the emission intensities after the addition of D-glucose, suggesting that interactions between **3** and D-glucose are insignificant under these conditions (Figure S32 and S35). However, addition of D-glucose to of a solution of **3** in 35% DMSO/0.012 M phosphate buffer at pH 8.5 induced a notable increase in both UV-vis absorbance and fluorescence intensities, and these remained unchanged over a period of four hours (Figure S37 and S38). Therefore, we further investigated the binding affinity of receptor **3** for D-glucose, D-fructose, and D-mannose in 35% DMSO/0.012 M phosphate buffer at pH 8.5.

At pH 8.5, compound **3** displayed two strong UV-vis absorbance bands in the 300-400 nm and 550-700 nm ranges, in 35% DMSO/0.012 M phosphate buffer. As illustrated in Figure 5a, the intensity of the absorption band at 550-700 nm

increases upon addition of increasing amounts of D-glucose (0–83 mM). Similarly, a considerable enhancement in the fluorescence intensity of **3** was observed when exciting at 645 nm (Figure 5b). The binding constant, K_a , was calculated from both UV-vis and fluorescence titration data for a 1:1 stoichiometric binding model, and the two K_a values matched

well, i.e. $K_a = 71 \text{ M}^{-1}$ and 70 M^{-1} , respectively (Figures S47–48). Most glucose monitoring systems have poor reliability/accuracy:⁸² the close agreement between the two independent detection techniques demonstrated herein supports reliable binding characteristics for the diboronic acid **3** with glucose.^{18,24,25}

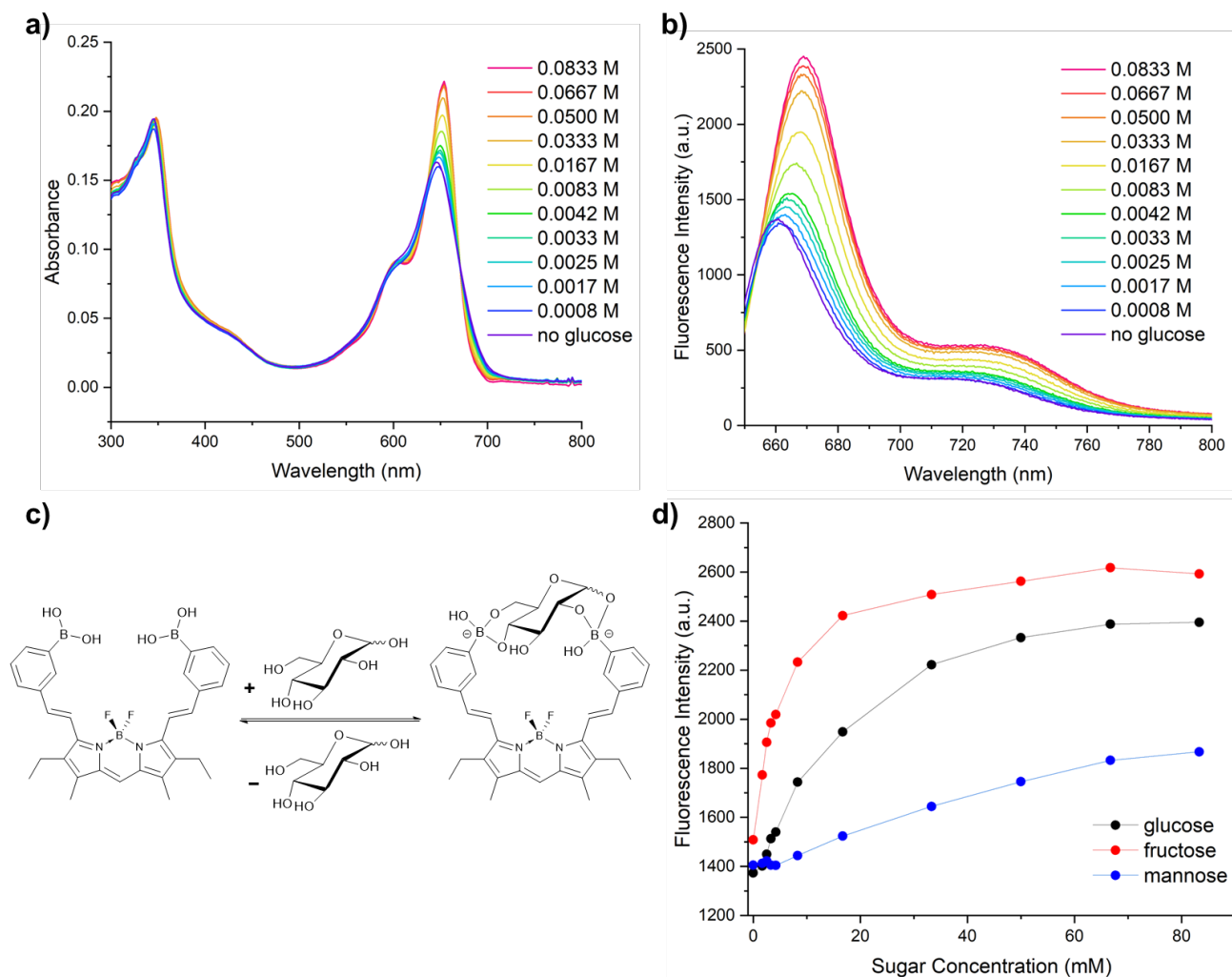


Figure 5 (a) Absorbance spectra of solutions of compound **3** in 35% DMSO/sodium phosphate buffer at pH 8.5 without D-glucose and with varying concentrations of D-glucose added. (b) Fluorescence spectra of compound **3** in 35% DMSO/sodium phosphate buffer at pH 8.5 when excited at 645 nm without D-glucose and with varying concentrations of D-glucose added. (c) Schematic illustration of 1:1 stoichiometric binding model for **3** and α -D-glucopyranose. (d) Turn-on change in emission maximum of solutions of **3** in 35% DMSO/sodium phosphate buffer at pH 8.5 with increasing amounts of D-glucose, D-fructose and D-mannose added when excited at 645 nm.

An increase in both the absorbance and fluorescence intensities was observed for addition of both D-fructose and D-mannose to diboronic acid **3** (Figures S43–44 and S45–46 respectively). The fluorescence enhancement of compound **3** with increasing amounts of D-glucose, D-fructose and D-mannose is shown in Figure 5d. Binding constants for D-fructose and D-mannose were also calculated from UV-vis and fluorescence titration data (Figures S49–50 and S51–52, respectively). The binding constant, K_a , for D-fructose was found to be much higher ($K_a = 410 \text{ M}^{-1}$) than for D-glucose, while D-mannose exhibited a lower binding affinity with a binding constant of $K_a = 16 \text{ M}^{-1}$. The binding affinities of **3** for D-glucose, D-fructose and D-mannose were compared to those reported

for published compounds that were similarly evaluated via analysis of emission data (Table 2). Notwithstanding the variations across experimental conditions, including buffer, co-solvent(s) and pH, the turn-on emissive carbohydrate sensing abilities of **3** compare well to previously published chromophores. Presumably courtesy of the extended π -conjugated framework, the diboronic acid **3** emits at wavelengths significantly bathochromically shifted cf. the other fluorescent frameworks. Similarly to **3**, phenyl boronic acid⁸³ and the BODIPY-appended monoboronic acid **gBBB3**⁵⁴ exhibit stronger affinity for D-fructose than for D-glucose. The chromophoric properties and the rigidity of the chemical framework are both affected by conformational flexibility, thus

affording an interplay between binding affinities and emission wavelengths/intensities that is attuned across the compounds presented in **Table 2** and remains at the heart of useful sensing using small molecules.

Table 2 Binding affinities of **3** and reported compounds

Compound	λ_{em} (nm)	Binding Constant K_a (M^{-1})		
		D-glucose	D-fructose	D-mannose
3	662	70	410	16
^a gBBB 3 ⁵⁴	504	18	920	-
7a (P-DBA) ³⁸	427	3844	423	110
Mc-CDBA ⁴²	457	710	180	62
Ca-CDBA ⁴²	438	4500	850	210
DPAC 1 ³⁷	592 ^b	816	1927	395

^amono-boronic acid; ^bhypsochromic shift to 452 nm upon D-glucose complexation

Taking these data and the various possibilities for complexation⁸⁴ into consideration, DFT calculations were used to reassess the 1:1 sensor:glucose binding motifs for **3** with D-glucose, compared to the relative binding energy of 0.0 kcal/mol for Drueckhammer's complex-1'. In addition to considering the α -D-glucopyranose complexed to the two boronic atoms through the 1,2- and 4,6-positions (Figures 2 and 5c), we considered diastereomeric possibilities and various α -pyranose and α -furanose forms. As shown in Figure 2b, the boron atoms of **3** become stereogenic upon complexation with glucose. In Figure 2b the three tetrahedrally (T) arranged binding sites at boron are labelled T1, T2 and T3, where T1 and T2 are the coordination sites of boron shown interacting with the oxygen atoms linked to C4 and C6 of α -D-glucopyranose, respectively. The diastereoisomer that instead results from complexation of the C6 oxygen atom of **3** at T3 (and not at T2) is listed as **P46b** in Table 3, and was calculated to be less stable than the originally-minimised diastereoisomer: "P" represents "pyranose", and "46" indicates complexation through oxygen atoms at C4 and C6 of the sugar. Various modes of complexation for α -D-glucopyranoses were also considered, and the relative calculated binding affinities are listed in Table 3 where "F" represents "furanose" and the oxygen atoms invoked in binding are indicated for each isomer. The corresponding minimised structures are presented in Figures S19-24.

Table 3 Calculated relative binding energies of **3** to D-glucose in pyranose and furanose forms

Entry	Isomer ^a	Form of D-glucose	Binding mode	Calculated binding affinity ^b (kcal/mol)
1	3 ^c	α -pyranose	1,2- and 4,6-	-2.3
2	P46b	α -pyranose	1,2- and 4,6-	0.9
3	F35a	α -furanose	1,2- and 3,5	-4.5
4	F35b	α -furanose	1,2- and 3,5	-5.9
5	F56a	α -furanose	1,2- and 5,6	-7.2
6	F56b	α -furanose	1,2- and 5,6	-2.5
7	F356b ^d	α -furanose	1,2- and 3,5,6	2.9

^aletters "a" and "b" indicate diastereomers courtesy of complexation at the boron bound to oxygen via the 3-/4-/5-/6- positions of glucose; ^bc.f. 0.0 kcal/mol for complex-1'; ^ccomplex-3' = **P46a**; ^donly one diastereomer minimised for complexes

resulting from interaction of α -D-glucopyranose with **3** through the oxygen atoms at C3, C5 and C6

We planned the design of **3** by building on previous work centred around complexation of bisboronic acids to α -D-glucopyranose (Figure 2). Clearly, this isomer is predicted, according to calculation, to be a more efficient binder than the diastereomeric form resulting via stereogenicity at boron (compare entries 1 and 2 in Table 3). However, and in contrast to literature reports relevant to other boronic acids that bind to glucose,⁸⁵ complexation of **3** via binding to oxygen atoms at C3, C5 and C6 of the α -furanose form of glucose is significantly less stable (Table 3, entry 7): intriguingly, our calculations predict that binding to α -D-glucopyranose via complexation of oxygen atoms at C3 and C5, or at C5 and C6, and/or via either diastereomer at boron, results in more efficient binding (compare Table 3 entries 3-6 c.f. entry 7). Again notwithstanding the variations in conditions between experiment and theory, these results suggest significant room for optimisation in the design of small molecule glucose binders/sensors with efficient binding properties and usable optochromic properties. Furthermore, these results highlight the need for detailed structural characterisation of the binder-sugar interaction amid various,^{85,86} and often contrasting, literature reports. Factors that influence binding, and thus the effectiveness and selectivity of sensors for carbohydrates, should include pyranose vrs. furanose isomers, ring size/puckering and diastereomeric binding options at boron created by complexation via different oxygen atoms of the sugar, and ring structure at boron depending on whether two or three oxygen atoms from the carbohydrate are involved in complexation at each boron atom.

NMR Studies

Nuclear magnetic resonance (NMR) spectroscopy is a commonly used method for monitoring the pKa values of boronic acids and their binding to carbohydrates.⁸⁷⁻⁸⁹ The methodology to determine the binding constant of phenylboronic acid with glucose by ¹H NMR is well established.⁸⁷ Such NMR titration experiments for binding glucose by phenylboronic acid can be performed in aqueous buffer solution courtesy of the suitable solubility of properties. Despite capably reproducing these binding constant values⁸⁷ for phenylboronic acid (Figure S53, Table S2), the insolubility of diboronic acids **2** and **3** in aqueous buffer required modification of the procedure to include a co-solvent. Using 80% methanol/phosphate buffer resulted in spectra with improved signals, yet the experiments were unreliable due to the low solubility of the diboronic acids (Figures S54-56). The use of DMSO as a co-solvent for this system was constrained by the suppression limitations of the NMR instrument. This lack of detailed NMR analysis, ideally needed to complement the absorption/emission changes corresponding to binding, prevents detailed understanding of sensor-glucose interactions and limits progress in the field. Furthermore, challenges collecting data across systems with matching solvent, buffer, concentrations and pH further limit acquisition of a complete

understanding regarding binding and perhaps lies at the heart of why carbohydrate probes are typically reported with just one mode of analysis.

Cell Staining Studies

Given the successful demonstration of BODIPYs α -appended with distyryl-linked aryl diboronic acids binding to carbohydrates, we sought to determine whether **2** and **3** could permeate cell membranes and stain live cells. Previous reports of sugar- or BODIPY-based fluorescent dyes for live-cell staining have used adherent and suspension cells incubated with the dyes for 1–2 hr at concentrations ranging from 1–100 μM .^{90–93} For our cell-staining experiments, we used HS578T cells, i.e. from an adherent epithelial breast cancer cell line, and assessed staining with BODIPY diboronic acids **2** and **3**, and the controls **4** and **5**, by fluorescence microscopy, flow cytometry and confocal microscopy. Initial fluorescence microscopy experiments, staining with **2** and **3** on live HS578T cells, demonstrated that increasing concentrations of **2** and **3** resulted in stronger cell staining (excitation 555 nm, emission 565 nm) with moderate staining at 10 μM and strong staining at 100 μM (Figure S59A–B). Treatment of cells with **4** and **5** at concentrations of 0.1–10 μM did not result in strong staining, although fluorescence beyond background was observed with 100 μM of **4** and **5** (Figure S59C–D): these results support the essential role of the boronic acid units. The nuclear DAPI (4',6-diamidino-2-phenylindole) co-stain did not have a major effect on the fluorescent signal of compounds **2–5** (excitation 358 nm, emission 461 nm).

HS578T cells were similarly treated with 0.1–100 μM **2–5** and the fluorescence intensity was quantified by flow cytometry (Figure 6A–E). Significant staining above background was observed for **2** and **3** at 0.1 μM , whereas control compounds **4** and **5** did not stain cells (Figures 6A, 6B and S60A). As the concentration of **2–5** was increased from 1–100 μM , the staining intensity (median fluorescence intensity, MFI) also increased (Figures 6A, 6C–E and S60B–D). At concentrations 10 μM or less, **2** and **3** resulted in greater MFI values than the controls **4** and **5** (Figures 6A, 6B–D and S60A–C), indicating the greater ability of the boronic acid-appended dyes to stain cells. However, at the highest concentration assessed (100 μM) all compounds **2–5** had very high MFIs, making it difficult to observe differences between the diboronic acids and the controls, likely as a result of non-specific staining with **4–5** (Figures 6A, 6D and S60D).

Since flow cytometry and fluorescence microscopy do not distinguish between intracellular and cell-surface staining, we sought to assess, using confocal microscopy, if dyes **2** and **3** were staining intracellularly. HS578T cells were treated with 10 μM of **2–5**. The corresponding fluorescence confocal microscopy images demonstrated that **2** moderately stains HS578T cells intracellularly and **3** strongly stains intracellularly (Figure 6F). The control compounds **4** and **5** showed limited intracellular staining at 10 μM , and staining was primarily observed on the cell surface. Notably, less fluorescence was observed using confocal microscopy (Figure 6F) compared to when using flow cytometry (Figure 6A). This is unsurprising given that flow cytometry detects fluorescence of the whole cell, whereas

confocal microscopy builds an image from individual slices across the cell, each of which inherently provides less fluorescence per slice.⁹⁴ Overall, based on the cell-staining data, compounds **2** and **3** appear to capably stain live cells intracellularly after incubation at 0.1–10 μM in 1% BSA in PBS for 2 hr at 37°C.

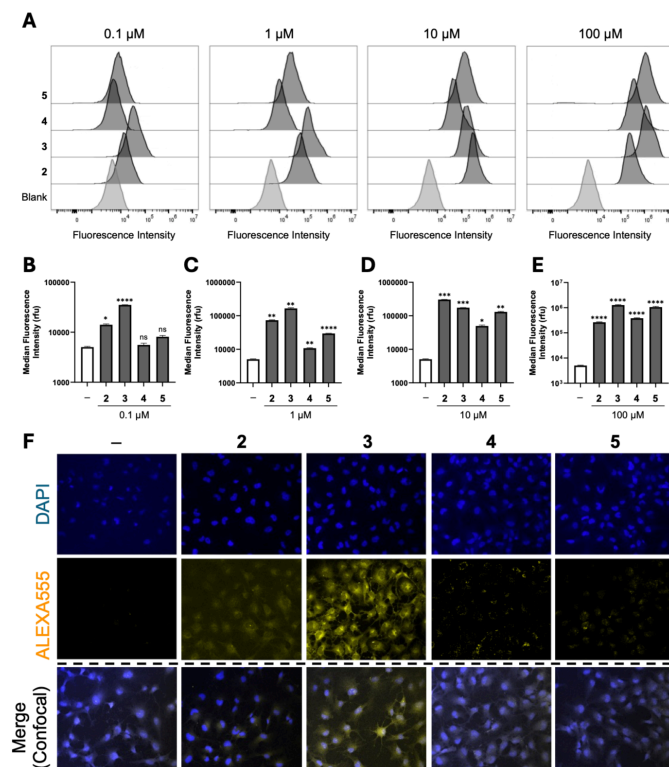


Figure 6. A. Histograms of HS578T cells stained with **2–5** (0.1–100 μM in 1% BSA in PBS, 2 hr, 37°C). Flow cytometry fluorescence data collected with the ECD-A channel (excitation 561 nm, emission 610 nm, N=3). B–E. Median fluorescence intensities (MFIs) of HS578T cells stained with **2–5** (0.1–100 μM in 1% BSA in PBS, 2 hr, 37°C). Flow cytometry fluorescence data collected with the ECD channel (excitation 561 nm, emission 610 nm, N=3). Statistical significance was assessed by one-way ANOVA relative to the blank control. ns = not significant $p \geq 0.05$; * $p < 0.05$; ** $p < 0.01$; *** $p < 0.001$; **** $p < 0.0001$. F. Confocal microscopy images of cells stained with 10 μM **2–5**. DAPI = 358 nm excitation, 461 nm emission. ALEXA555 = 555 nm excitation, 565 nm emission.

Conclusions

In summary, a synthetic route to two symmetrical BODIPYs that bind carbohydrates is described. Determination of the crystal structures showed that the boronic acid moieties link to the BODIPY fluorophore core via rigid styryl linkers and thereby create a confined geometry for 1:1 binding to carbohydrates. DFT calculations predicted that the meta-substituted analogue **3** would exhibit the most favourable binding, and this was corroborated via titration experiments. The results of UV-vis and fluorescence titration experiments indicate that the bisboronic acid **3** binds to sugars in a 1:1 mode, matching the design principles used. Supporting NMR titration experiments were hampered by low solubility of **2** and **3**, thereby perhaps offering insight into the reasons why studies involving small-molecule carbohydrate sensors are often published with

minimal data regarding the mode of binding. The BODIPYs **2** and **3**, α -appended with distyryl-linked aryl diboronic acids, were shown to stain HS578T cells intracellularly with emission signals correlating to their concentration. BODIPY **3** exhibits significant fluorescence enhancement upon binding to D-glucose, D-fructose and D-mannose, thereby supporting the introduction of this framework as a potential probe for selective sensing of carbohydrates. Next steps will involve building on the key design features such that synthetic modifications of the dye framework improve solubility and enable careful tuning to meet carbohydrate binding characteristics.

Author Contributions

Conceptualisation: AT and DLJ

Funding acquisition: AT and CJC

Investigation: AA, JMK, ECS, DN, KNR, ERJ

Project administration: AT

Supervision: AT, DLJ and CJC

Writing – original drafts: AA, ECS, JMK, KNR, CJC and ERJ

Writing – review & editing: AA, AT, KNR, CJC, DLJ, ERJ and AT

Conflicts of interest

There are no conflicts to declare.

Acknowledgements

This work was supported by NSERC of Canada via Discovery Grants and the CREATE Training Program in BioActives (510963). This work was supported, in part, thanks to funding from the Canada Research Chairs Program (funding reference number 950-232829). This research was enabled, in part, by funding from the Canada Foundation for Innovation (JELF 39824) and Research Nova Scotia (Research Opportunities Fund 2020-1208). J.M.K. acknowledges NSERC for a Vanier CGS. We thank Dr. Michael Lumsden and Mr. Xiao Feng (both at Dalhousie University) for sharing their expertise in NMR spectroscopy and mass spectrometry, respectively.

References

- Galan, M. C.; Benito-Alifonso, D.; Watt, G. M. Carbohydrate Chemistry in Drug Discovery. *Org. Biomol. Chem.* **2011**, *9* (10), 3598–3610.
- Varki, A. Biological Roles of Glycans. *Glycobiology* **2017**, *27* (1), 3–49.
- Wang, J.; Zhang, Y.; Lu, Q.; Xing, D.; Zhang, R. Exploring Carbohydrates for Therapeutics: A Review on Future Directions. *Front. Pharmacol.* **2021**, *12*.
- Clemente-Suárez, V. J.; Mielgo-Ayuso, J.; Martín-Rodríguez, A.; Ramos-Campo, D. J.; Redondo-Flórez, L.; Tornero-Aguilera, J. F. The Burden of Carbohydrates in Health and Disease. *Nutrients* **2022**, *14* (18).
- Dai, C.; Sagwal, A.; Cheng, Y.; Peng, H.; Chen, W.; Wang, B. Carbohydrate Biomarker Recognition Using Synthetic Lectin Mimics. *Pure Appl. Chem.* **2012**, *84* (11), 2479–2498.
- Sun, X.; Zhai, W.; Fossey, J. S.; James, T. D. Boronic Acids for Fluorescence Imaging of Carbohydrates. *Chem. Commun.* **2016**, *52* (17), 3456–3469.
- Tan, Y.; Wu, J.; Song, L.; Zhang, M.; Hipolito, C. J.; Wu, C.; Wang, S.; Zhang, Y.; Yin, Y. Merging the Versatile Functionalities of Boronic Acid with Peptides. *Int. J. Mol. Sci.* **2021**, *22* (23).
- Abrantes-Coutinho, V. E.; Santos, A. O.; Moura, R. B.; Pereira-Junior, F. N.; Mascaró, L. H.; Morais, S.; Oliveira, T. M. B. F. Systematic Review on Lectin-Based Electrochemical Biosensors for Clinically Relevant Carbohydrates and Glycoconjugates. *Colloids Surf. B. Biointerfaces* **2021**, *208*, 112148.
- Steiner, M.-S.; Duerkop, A.; Wolfbeis, O. S. Optical Methods for Sensing Glucose. *Chem. Soc. Rev.* **2011**, *40* (9), 4805–4839.
- Ahmed, I.; Jiang, N.; Shao, X.; Elsherif, M.; Alam, F.; Salih, A.; Butt, H.; Yetisen, A. K. Recent Advances in Optical Sensors for Continuous Glucose Monitoring. *Sens. Diagn.* **2022**, *1* (6), 1098–1125.
- Wang, H.-C.; Lee, A.-R. Recent Developments in Blood Glucose Sensors. *J. Food Drug Anal.* **2015**, *23* (2), 191–200.
- Hansen, J. S.; Christensen, J. B. Recent Advances in Fluorescent Arylboronic Acids for Glucose Sensing. *Biosensors* **2013**, *3* (4), 400–418.
- Wu, X.; Chen, X.-X.; Jiang, Y.-B. Recent Advances in Boronic Acid-Based Optical Chemosensors. *Analyst* **2017**, *142* (9), 1403–1414.
- Fang, G.; Wang, H.; Bian, Z.; Sun, J.; Liu, A.; Fang, H.; Liu, B.; Yao, Q.; Wu, Z. Recent Development of Boronic Acid-Based Fluorescent Sensors. *RSC Adv.* **2018**, *8* (51), 29400–29427.
- Nan, K.; Jiang, Y.-N.; Li, M.; Wang, B. Recent Progress in Diboronic-Acid-Based Glucose Sensors. *Biosensors* **2023**, *13* (6).
- Elsherif, M.; Hassan, M. U.; Yetisen, A. K.; Butt, H. Glucose Sensing with Phenylboronic Acid Functionalized Hydrogel-Based Optical Diffusers. *ACS Nano* **2018**, *12* (3), 2283–2291.
- Melavanki, R.; Kusanur, R.; Sadasivuni, K. K.; Singh, D.; Patil, N. R. Investigation of Interaction between Boronic Acids and Sugar: Effect of Structural Change of Sugars on Binding Affinity Using Steady State and Time Resolved Fluorescence Spectroscopy and Molecular Docking. *Heliyon* **2020**, *6* (10), e05081.
- Hashemzadeh, T.; Haghighatbin, M. A.; Agugiaro, J.; Wilson, D. J. D.; Hogan, C. F.; Barnard, P. J. Luminescent Iridium(III)-Boronic Acid Complexes for Carbohydrate Sensing. *Dalton Trans.* **2020**, *49* (32), 11361–11374.
- Sugita, K.; Suzuki, Y.; Tsuchido, Y.; Fujiwara, S.; Hashimoto, T.; Hayashita, T. A Simple Supramolecular Complex of Boronic Acid-Appended β -Cyclodextrin and a Fluorescent Boronic Acid-Based Probe with Excellent Selectivity for d-Glucose in Water. *RSC Adv.* **2022**, *12* (31), 20259–20263.
- Sugita, K.; Tsuchido, Y.; Kasahara, C.; Casulli, M. A.; Fujiwara, S.; Hashimoto, T.; Hayashita, T. Selective Sugar Recognition by Anthracene-Type Boronic Acid Fluorophore/Cyclodextrin Supramolecular Complex Under Physiological pH Condition. *Front. Chem.* **2019**, *7*.
- Wang, B.; Chou, K.-H.; Queenan, B. N.; Pennathur, S.; Bazan, G. C. Molecular Design of a New Diboronic Acid for the Electrohydrodynamic Monitoring of Glucose. *Angew. Chem., Int. Ed. Engl.* **2019**, *58* (31), 10612–10615.
- Ndebele, N.; Mack, J.; Nyokong, T. A 3,5-DistyrylBODIPY Dye Functionalized with Boronic Acid Groups for Direct Electrochemical Glucose Sensing. *Electroanalysis* **2019**, *31* (1), 137–145.

- (23) Axthelm, J.; Görls, H.; Schubert, U. S.; Schiller, A. Fluorinated Boronic Acid-Appended Bipyridinium Salts for Diol Recognition and Discrimination via 19F NMR Barcodes. *J. Am. Chem. Soc.* **2015**, *137* (49), 15402–15405.
- (24) Guo, L.-E.; Hong, Y.; Zhang, S.-Y.; Zhang, M.; Yan, X.-S.; Cao, J.-L.; Li, Z.; James, T. D.; Jiang, Y.-B. Proline-Based Boronic Acid Receptors for Chiral Recognition of Glucose. *J. Org. Chem.* **2018**, *83* (24), 15128–15135.
- (25) Gao, X.; Du, X.; Shi, Y. A Bisboronic Acid Sensor for Ultra-High Selective Glucose Assay by 19F NMR Spectroscopy. *Anal. Chem.* **2021**, *93* (19), 7220–7225.
- (26) Gao, Z. F.; Ogbe, A. Y.; Sann, E. E.; Wang, X.; Xia, F. Turn-on Fluorescent Sensor for the Detection of Glucose Using Manganese Dioxide-phenol Formaldehyde Resin Nanocomposite. *Talanta* **2018**, *180*, 12–17.
- (27) Du, P.; Niu, Q.; Chen, J.; Chen, Y.; Zhao, J.; Lu, X. “Switch-On” Fluorescence Detection of Glucose with High Specificity and Sensitivity Based on Silver Nanoparticles Supported on Porphyrin Metal–Organic Frameworks. *Anal. Chem.* **2020**, *92* (11), 7980–7986.
- (28) Liu, S.; Lv, C.; Liu, R.; Yang, G.; Li, S.; Zuo, L.; Xue, P. A Label-Free “Turn-on” Fluorescence Platform for Glucose Based on AuNCs@MnO₂ Nanocomposites. *New J. Chem.* **2019**, *43* (33), 13143–13151.
- (29) Guo, Z.; Shin, I.; Yoon, J. Recognition and Sensing of Various Species Using Boronic Acid Derivatives. *Chem. Commun.* **2012**, *48* (48), 5956–5967.
- (30) Wu, X.; Li, Z.; Chen, X.-X.; Fossey, J. S.; James, T. D.; Jiang, Y.-B. Selective Sensing of Saccharides Using Simple Boronic Acids and Their Aggregates. *Chem. Soc. Rev.* **2013**, *42* (20), 8032–8048.
- (31) Bull, S. D.; Davidson, M. G.; van den Elsen, J. M. H.; Fossey, J. S.; Jenkins, A. T. A.; Jiang, Y.-B.; Kubo, Y.; Marken, F.; Sakurai, K.; Zhao, J.; James, T. D. Exploiting the Reversible Covalent Bonding of Boronic Acids: Recognition, Sensing, and Assembly. *Acc. Chem. Res.* **2013**, *46* (2), 312–326.
- (32) Zhai, W.; Sun, X.; James, T. D.; Fossey, J. S. Boronic Acid-Based Carbohydrate Sensing. *Asian J. Chem.* **2015**, *10* (9), 1836–1848.
- (33) Zhang, X.; Liu, G.; Ning, Z.; Xing, G. Boronic Acid-Based Chemical Sensors for Saccharides. *Carbohydr. Res.* **2017**, *452*, 129–148.
- (34) James, T. D.; Sandanayake, K. R. A. S.; Iguchi, R.; Shinkai, S. Novel Saccharide-Photoinduced Electron Transfer Sensors Based on the Interaction of Boronic Acid and Amine. *J. Am. Chem. Soc.* **1995**, *117* (35), 8982–8987.
- (35) Arimori, S.; Bell, M. L.; Oh, C. S.; Frimat, K. A.; James, T. D. Modular Fluorescence Sensors for Saccharides. *Chem. Commun.* **2001**, No. 18, 1836–1837.
- (36) Arimori, S.; Bell, M. L.; Oh, C. S.; Frimat, K. A.; James, T. D. Modular Fluorescence Sensors for Saccharides. *J. Chem. Soc., Perkin Trans. 1* **2002**, No. 6, 803–808.
- (37) Ramos-Soriano, J.; Benitez-Benitez, S. J.; Davis, A. P.; Galan, M. C. A Vibration-Induced-Emission-Based Fluorescent Chemosensor for the Selective and Visual Recognition of Glucose. *Angew. Chem. Int. Ed.* **2021**, *60* (31), 16880–16884.
- (38) Wang, K.; Zhang, R.; Yue, X.; Zhou, Z.; Bai, L.; Tong, Y.; Wang, B.; Gu, D.; Wang, S.; Qiao, Y.; Liu, Q.; Xue, X.; Yin, Y.; Xi, R.; Meng, M. Synthesis of Diboronic Acid-Based Fluorescent Probes for the Sensitive Detection of Glucose in Aqueous Media and Biological Matrices. *ACS Sens.* **2021**, *6* (4), 1543–1551.
- (39) Solomos, K.; Tarus, V.; Kotek, V.; Invernizzi, G.; Hoeg-Jensen, T. Diboronate Fluorophore for the Measurement of L-Glucose and Other Carbohydrates and Its Interaction with Albumin. *ACS Omega* **2022**, *7* (28), 24662–24668.
- (40) Ohno, Y.; Tanaka, R.; Suzuki, Y.; Sugaya, T.; Iwatsuki, S.; Inamo, M.; Ishihara, K. Detailed Reaction Mechanism of Bis-(o-Aminomethylphenylboronic Acid)-Based Receptors with Various Length Methylene-Chain Linkers with D-Glucose. *ChemistrySelect* **2022**, *7* (29), e202200603.
- (41) Valdes-García, J.; Zamora-Moreno, J.; Salomón-Flores, M. K.; Martínez-Otero, D.; Barroso-Flores, J.; Yatsimirsky, A. K.; Bazany-Rodríguez, I. J.; Dorazco-González, A. Fluorescence Sensing of Monosaccharides by Bis-Boronic Acids Derived from Quinolinium Dicarboxamides: Structural and Spectroscopic Studies. *J. Org. Chem.* **2023**, *88* (4), 2174–2189.
- (42) Wang, K.; Zhang, R.; Zhao, X.; Ma, Y.; Ren, L.; Ren, Y.; Chen, G.; Ye, D.; Wu, J.; Hu, X.; Guo, Y.; Xi, R.; Meng, M.; Yao, Q.; Li, P.; Chen, Q.; James, T. D. Reversible Recognition-Based Boronic Acid Probes for Glucose Detection in Live Cells and Zebrafish. *J. Am. Chem. Soc.* **2023**, *145* (15), 8408–8416.
- (43) Yang, W.; He, H.; Drueckhammer, D. G. Computer-Guided Design in Molecular Recognition: Design and Synthesis of a Glucopyranose Receptor. *Angew. Chem. Int. Ed.* **2001**, *40* (9), 1714–1718.
- (44) Loudet, A.; Burgess, K. BODIPY Dyes and Their Derivatives: Syntheses and Spectroscopic Properties. *Chem. Rev.* **2007**, *107* (11), 4891–4932.
- (45) Beh, M. H. R.; Douglas, K. I. B.; House, K. T. E.; Murphy, A. C.; Sinclair, J. S. T.; Thompson, A. Robust Synthesis of F-BODIPYs. *Org. Biomol. Chem.* **2016**, *14* (48), 11473–11479.
- (46) Lu, H.; Mack, J.; Yang, Y.; Shen, Z. Structural Modification Strategies for the Rational Design of Red/NIR Region BODIPYs. *Chem. Soc. Rev.* **2014**, *43* (13), 4778–4823.
- (47) Hansen, J. S.; Hoeg-Jensen, T.; Christensen, J. B. Redemitting BODIPY Boronic Acid Fluorescent Sensors for Detection of Lactate. *Tetrahedron* **2017**, *73* (21), 3010–3013.
- (48) Hansen, J. S.; Ficker, M.; Petersen, J. F.; Christensen, J. B.; Hoeg-Jensen, T. Ortho-Substituted Fluorescent Aryl Monoboronic Acid Displays Physiological Binding of d-Glucose. *Tetrahedron Lett.* **2013**, *54* (14), 1849–1852.
- (49) Hansen, J. S.; Petersen, J. F.; Hoeg-Jensen, T.; Christensen, J. B. Buffer and Sugar Concentration Dependent Fluorescence Response of a BODIPY-Based Aryl Monoboronic Acid Sensor. *Tetrahedron Lett.* **2012**, *53* (44), 5852–5855.
- (50) Zhai, J.; Pan, T.; Zhu, J.; Xu, Y.; Chen, J.; Xie, Y.; Qin, Y. Boronic Acid Functionalized Boron Dipyrromethene Fluorescent Probes: Preparation, Characterization, and Saccharides Sensing Applications. *Anal. Chem.* **2012**, *84* (23), 10214–10220.
- (51) DiCesare, N.; Lakowicz, J. R. Fluorescent Probe for Monosaccharides Based on a Functionalized Boron-Dipyrromethene with a Boronic Acid Group. *Tetrahedron Lett.* **2001**, *42* (52), 9105–9108.
- (52) Ashokkumar, P.; Bell, J.; Buurman, M.; Rurack, K. Analytical Platform for Sugar Sensing in Commercial Beverages Using a Fluorescent BODIPY “Light-up” Probe. *Sens. Actuators B Chem.* **2018**, *256*, 609–615.
- (53) Cheruthu, N. M.; Komatsu, T.; Ueno, T.; Hanaoka, K.; Urano, Y. Development of Ratiometric Carbohydrate Sensor Based on Boron Dipyrromethene (BODIPY) Scaffold. *Bioorg. Med. Chem. Lett.* **2019**, *29* (22), 126684.
- (54) Hoffmann, C.; Jourdain, M.; Grandjean, A.; Titz, A.; Jung, G. β -Boronic Acid-Substituted Bodipy Dyes for Fluorescence

- Anisotropy Analysis of Carbohydrate Binding. *Anal. Chem.* **2022**, *94* (16), 6112–6119.
- (55) Liu, B.; Novikova, N.; Simpson, M. C.; Timmer, M. S. M.; Stocker, B. L.; Söhnel, T.; Ware, D. C.; Brothers, P. J. Lighting up Sugars: Fluorescent BODIPY–Gluco-Furanose and –Septanose Conjugates Linked by Direct B–O–C Bonds. *Org. Biomol. Chem.* **2016**, *14* (23), 5205–5209.
- (56) Kanyan, D.; Horacek-Glading, M.; Wildervanck, M. J.; Söhnel, T.; Ware, D. C.; Brothers, P. J. O-BODIPYs as Fluorescent Labels for Sugars: Glucose, Xylose and Ribose. *Org. Chem. Front.* **2022**, *9* (3), 720–730.
- (57) Ansteatt, S.; Meares, A.; Ptaszek, M. Amphiphilic Near-IR-Emitting 3,5-Bis(2-Pyrrolylethenyl)BODIPY Derivatives: Synthesis, Characterization, and Comparison with Other (Hetero)Arylethenyl-Substituted BODIPYs. *J. Org. Chem.* **2021**, *86* (13), 8755–8765.
- (58) Dost, Z.; Atilgan, S.; Akkaya, E. U. Distyryl-Boradiazaindacenes: Facile Synthesis of Novel near IR Emitting Fluorophores. *Tetrahedron* **2006**, *62* (36), 8484–8488.
- (59) Deniz, E.; Isbasar, G. C.; Bozdemir, Ö. A.; Yildirim, L. T.; Siemiarczuk, A.; Akkaya, E. U. Bidirectional Switching of Near IR Emitting Boradiazaindacene Fluorophores. *Org. Lett.* **2008**, *10* (16), 3401–3403.
- (60) Yang, J.; Cai, F.; Desbois, N.; Huang, L.; Gros, C. P.; Bolze, F.; Fang, Y.; Wang, S.; Xu, H.-J. Synthesis, Spectroscopic Characterization, One and Two-Photon Absorption Properties and Electrochemistry of π -Expanded BODIPYs Dyes. *Dyes Pigm.* **2020**, *175*, 108173.
- (61) James, T. D.; Sandanayake, K. R. A. S.; Shinkai, S. A Glucose-Selective Molecular Fluorescence Sensor. *Angew. Chem., Int. Ed. Engl.* **1994**, *33* (21), 2207–2209.
- (62) Vydrov, O. A.; Scuseria, G. E. Assessment of a Long-Range Corrected Hybrid Functional. *J. Chem. Phys.* **2006**, *125* (23), 234109.
- (63) Johnson, E. R.; Otero-de-la-Roza, A.; Dale, S. G.; DiLabio, G. A. Efficient Basis Sets for Non-Covalent Interactions in XDM-Corrected Density-Functional Theory. *J. Chem. Phys.* **2013**, *139* (21), 214109.
- (64) Johnson, E. R. The Exchange-Hole Dipole Moment Dispersion Model. In *Interactions in Quantum Chemistry and Physics*; Otero-de-la Roza, A., DiLabio, G. A., Eds.; Elsevier, 2017; pp 169–194.
- (65) Kwon, H.-Y.; Liu, X.; Choi, E. G.; Lee, J. Y.; Choi, S.-Y.; Kim, J.-Y.; Wang, L.; Park, S.-J.; Kim, B.; Lee, Y.-A.; Kim, J.-J.; Kang, N. Y.; Chang, Y.-T. Development of a Universal Fluorescent Probe for Gram-Positive Bacteria. *Angew. Chem. Int. Ed.* **2019**, *58* (25), 8426–8431.
- (66) Kang, H.; Si, Y.; Liu, Y.; Zhang, X.; Zhang, W.; Zhao, Y.; Yang, B.; Liu, Y.; Liu, Z. Photophysical/Chemistry Properties of Distyryl-BODIPY Derivatives: An Experimental and Density Functional Theoretical Study. *J. Phys. Chem. A* **2018**, *122* (25), 5574–5579.
- (67) Yuen, A. K. L.; Hutton, C. A. Deprotection of Pinacolyl Boronate Esters via Hydrolysis of Intermediate Potassium Trifluoroborates. *Tetrahedron Lett.* **2005**, *46* (46), 7899–7903.
- (68) Pennington, T. E.; Kardiman, C.; Hutton, C. A. Deprotection of Pinacolyl Boronate Esters by Transesterification with Polystyrene–Boronic Acid. *Tetrahedron Lett.* **2004**, *45* (35), 6657–6660.
- (69) Lennox, A. J. J.; Lloyd-Jones, G. C. Selection of Boron Reagents for Suzuki–Miyaura Coupling. *Chem. Soc. Rev.* **2014**, *43* (1), 412–443.
- (70) Malan, C.; Morin, C.; Preckher, G. Two Reducible Protecting Groups for Boronic Acids. *Tetrahedron Lett.* **1996**, *37* (37), 6705–6708.
- (71) Sun, J.; Perfetti, M. T.; Santos, W. L. A Method for the Deprotection of Alkylpinacolyl Boronate Esters. *J. Org. Chem.* **2011**, *76* (9), 3571–3575.
- (72) Öztürk, D.; Ömeroğlu, İ.; Köksoy, B.; Göl, C.; Durmuş, M. A BODIPY Decorated Multiple Mode Reusable Paper-Based Colorimetric and Fluorometric pH Sensor. *Dyes Pigm.* **2022**, 110510.
- (73) Gibbs, J. H.; Zhou, Z.; Kessel, D.; Fronczek, F. R.; Pakhomova, S.; Vicente, M. G. H. Synthesis, Spectroscopic, and in Vitro Investigations of 2,6-Diiodo-BODIPYs with PDT and Bioimaging Applications. *J. Photochem. Photobiol. B: Biol.* **2015**, *145*, 35–47.
- (74) Tao, J.; Sun, D.; Sun, L.; Li, Z.; Fu, B.; Liu, J.; Zhang, L.; Wang, S.; Fang, Y.; Xu, H. Tuning the Photo-Physical Properties of BODIPY Dyes: Effects of 1, 3, 5, 7- Substitution on Their Optical and Electrochemical Behaviours. *Dyes Pigm.* **2019**, *168*, 166–174.
- (75) Peters, J. A. Interactions between Boric Acid Derivatives and Saccharides in Aqueous Media: Structures and Stabilities of Resulting Esters. *Coord. Chem. Rev.* **2014**, *268*, 1–22.
- (76) Brooks, W. L. A.; Deng, C. C.; Sumerlin, B. S. Structure–Reactivity Relationships in Boronic Acid–Diol Complexation. *ACS Omega* **2018**, *3* (12), 17863–17870.
- (77) Chatterjee, S.; Tripathi, N. M.; Bandyopadhyay, A. The Modern Role of Boron as a ‘Magic Element’ in Biomedical Science: Chemistry Perspective. *Chem. Commun.* **2021**, *57* (100), 13629–13640.
- (78) Furikado, Y.; Nagahata, T.; Okamoto, T.; Sugaya, T.; Iwatsuki, S.; Inamo, M.; Takagi, H. D.; Odani, A.; Ishihara, K. Universal Reaction Mechanism of Boronic Acids with Diols in Aqueous Solution: Kinetics and the Basic Concept of a Conditional Formation Constant. *Chem. Eur. J.* **2014**, *20* (41), 13194–13202.
- (79) Yan, J.; Springsteen, G.; Deeter, S.; Wang, B. The Relationship among pKa, pH, and Binding Constants in the Interactions between Boronic Acids and Diols—It Is Not as Simple as It Appears. *Tetrahedron* **2004**, *60* (49), 11205–11209.
- (80) Kurnia, K. A.; Setyaningsih, W.; Darmawan, N.; Yulianto, B. A Comprehensive Study on the Impact of the Substituent on pKa of Phenylboronic Acid in Aqueous and Non-Aqueous Solutions: A Computational Approach. *J. Mol. Liq.* **2021**, *326*, 115321.
- (81) Krämer, J.; Kang, R.; Grimm, L. M.; De Cola, L.; Picchetti, P.; Biedermann, F. Molecular Probes, Chemosensors, and Nanosensors for Optical Detection of Biorelevant Molecules and Ions in Aqueous Media and Biofluids. *Chem. Rev.* **2022**, *122* (3), 3459–3636.
- (82) Freckmann, G.; Pleus, S.; Grady, M.; Setford, S.; Levy, B. Measures of Accuracy for Continuous Glucose Monitoring and Blood Glucose Monitoring Devices. *J. Diabetes Sci. Technol.* **2019**, *13* (3), 575–583.
- (83) Ellis, G. A.; Palte, M. J.; Raines, R. T. Boronate-Mediated Biologic Delivery. *J. Am. Chem. Soc.* **2012**, *134* (8), 3631–3634.
- (84) Sun, X.; Chapin, B. M.; Metola, P.; Collins, B.; Wang, B.; James, T. D.; Anslyn, E. V. The Mechanisms of Boronate Ester Formation and Fluorescent Turn-on in Ortho-Aminomethylphenylboronic Acids. *Nat. Chem.* **2019**, *11* (9), 768–778.
- (85) Norrild, J. C.; Eggert, H. Evidence for Mono- and Bidentate Boronate Complexes of Glucose in the Furanose Form. Application of ¹JC–C Coupling Constants as a Structural Probe. *J. Am. Chem. Soc.* **1995**, *117* (5), 1479–1484.

- (86) James, T. D.; Sandanayake, K. R. A. S.; Shinkai, S. Novel Photoinduced Electron-Transfer Sensor for Saccharides Based on the Interaction of Boronic Acid and Amine. *J. Chem. Soc., Chem. Commun.* **1994**, No. 4, 477–478.
- (87) Ellis, G. A.; Palte, M. J.; Raines, R. T. Boronate-Mediated Biologic Delivery. *J. Am. Chem. Soc.* **2012**, *134* (8), 3631–3634.
- (88) Dowlut, M.; Hall, D. G. An Improved Class of Sugar-Binding Boronic Acids, Soluble and Capable of Complexing Glycosides in Neutral Water. *J. Am. Chem. Soc.* **2006**, *128* (13), 4226–4227.
- (89) Valenzuela, S. A.; Howard, J. R.; Park, H. M.; Darbha, S.; Anslyn, E. V. ¹¹B NMR Spectroscopy: Structural Analysis of the Acidity and Reactivity of Phenyl Boronic Acid–Diol Condensations. *J. Org. Chem.* **2022**, *87* (22), 15071–15076.
- (90) Ricardo, M. G.; Reuber, E. E.; Yao, L.; Danglad-Flores, J.; Delbianco, M.; Seeberger, P. H. Design, Synthesis, and Characterization of Stapled Oligosaccharides. *J. Am. Chem. Soc.* **2022**, *144* (40), 18429–18434.
- (91) Wijesooriya, C. S.; Peterson, J. A.; Shrestha, P.; Gehrman, E. J.; Winter, A. H.; Smith, E. A. A Photoactivatable BODIPY Probe for Localization-Based Super-Resolution Cellular Imaging. *Angew. Chem. Int. Ed.* **2018**, *57* (39), 12685–12689.
- (92) Wu, G.; Zeng, F.; Wu, S. A Water-Soluble and Specific BODIPY-Based Fluorescent Probe for Hypochlorite Detection and Cell Imaging. *Anal. Methods* **2013**, *5* (20), 5589–5596.
- (93) Zheng, Q.; Xu, G.; Prasad, P. N. Conformationally Restricted Dipyrromethene Boron Difluoride (BODIPY) Dyes: Highly Fluorescent, Multicolored Probes for Cellular Imaging. *Chem. Eur. J.* **2008**, *14* (19), 5812–5819.
- (94) Basiji, D. A.; Ortyu, W. E.; Liang, L.; Venkatachalam, V.; Morrissey, P. Cellular Image Analysis and Imaging by Flow Cytometry. *Clin. Lab. Med.* **2007**, *27* (3), 653–670.